

PCCP

Accepted Manuscript



This is an *Accepted Manuscript*, which has been through the Royal Society of Chemistry peer review process and has been accepted for publication.

Accepted Manuscripts are published online shortly after acceptance, before technical editing, formatting and proof reading. Using this free service, authors can make their results available to the community, in citable form, before we publish the edited article. We will replace this *Accepted Manuscript* with the edited and formatted *Advance Article* as soon as it is available.

You can find more information about *Accepted Manuscripts* in the [Information for Authors](#).

Please note that technical editing may introduce minor changes to the text and/or graphics, which may alter content. The journal's standard [Terms & Conditions](#) and the [Ethical guidelines](#) still apply. In no event shall the Royal Society of Chemistry be held responsible for any errors or omissions in this *Accepted Manuscript* or any consequences arising from the use of any information it contains.

*PCCP Perspective***The Single GUV Method for Revealing the Functions of Antimicrobial, Pore-Forming Toxin, and Cell-Penetrating Peptides or Proteins**

Md. Zahidul Islam,^a Jahangir Md. Alam,^b Yukihiro Tamba,^c Mohammad Abu Sayem Karal,^a and Masahito Yamazaki^{a, b, d, *}

^a*Integrated Bioscience Section, Graduate School of Science and Technology, Shizuoka University, Shizuoka, 422-8529, Japan,* ^b*Nanomaterials Research Division, Research Institute of Electronics, Shizuoka University, Shizuoka, 422-8529, Japan,* ^c*Suzuka National College of Technology, Suzuka, 510-0294, Japan,* and ^d*Dept. Physics, Graduate School of Science, Shizuoka University, Shizuoka, 422-8529, Japan.*

*Correspondence should be addressed to:

Dr. Masahito Yamazaki,

Nanomaterials Research Division, Research Institute of Electronics,

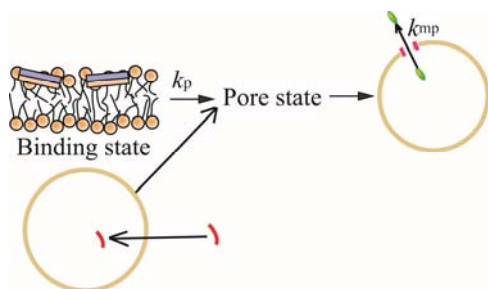
Shizuoka University

836 Oya, Suruga-ku, Shizuoka 422-8529, Japan

TEL and FAX: +81-54-238-4741

Email: spmyama@ipc.shizuoka.ac.jp

Table of contents entry



The single GUV method provides detailed information on the elementary processes of peptide/protein-induced pore formation in lipid membranes and the entry of peptide into a GUV; specifically, the GUV method provides the rate constants of these processes.

ABSTRACT

We recently developed the single giant unilamellar vesicle (GUV) method for investigating the functions and dynamics of biomembranes. The single GUV method can provide detailed information on the elementary processes of physiological phenomena in biomembranes, such as their rate constants. Here we describe the process of pore formation induced by the antimicrobial peptide (AMP), magainin 2, and the pore-forming toxin (PFT), lysenin, as revealed by the single GUV method. We obtained the rate constants of several elementary steps, such as peptide/protein-induced pore formation in lipid membranes and the membrane permeation of fluorescent probes through the pores. Information on the entry of the cell-penetrating peptide (CPP), transportan 10 (TP10), into a single GUV and its induced pore formation in lipid membranes was also obtained. We compare the single GUV method with other methods for investigating the interaction of peptides/proteins with lipid membranes (i.e., the large unilamellar vesicle (LUV) suspension method, the GUV suspension method, and single channel recording), and discuss the pros and cons of the single GUV method. On the basis of these data, we discuss the advantages of the single GUV method.

1. Introduction

Many physiologically active substances and drugs bind specifically with various membrane proteins in the plasma membrane, the outer membrane of cells, triggering biochemical reactions inside the cells. However, it was recently recognized that many peptides and proteins which damage the plasma membranes sufficiently seriously to kill the cell interact strongly with the lipid membrane regions. One of these peptides/proteins is antimicrobial peptide (AMP), which has both bactericidal and fungicidal activity. A wide variety of organisms, including amphibians, invertebrates, plants, and mammals, produce AMPs to defend themselves against microbes such as bacteria, fungi, viruses, and protozoa.^{1,2} However, AMPs have no or very low toxicity against cells of the organisms which produce AMPs (e.g., mammalian cells). The target of AMPs is believed to be the lipid regions of bacterial and fungal cellular membranes. Among the AMPs, magainin 2, which was first isolated from the African clawed frog *Xenopus laevis*,^{3,4} has been extensively investigated. All-D amino acid magainin 2 has the same antibacterial activity as that of natural, all-L amino acid magainin 2.⁵ Since specific interaction of magainin 2 with chiral receptors or proteins is not required for its antibacterial activity, this observation indicates that the target of magainin 2 is the lipid regions of bacterial and fungal biomembranes. Another example of these peptides/proteins is pore-forming toxin (PFT), which is produced by a wide variety of organisms, including bacteria and invertebrates.⁶⁻⁸ Most PFTs bind a specific lipid and create pores in the lipid regions of eukaryotic plasma membranes, thereby inducing cytolysis. On the other hand, cell-penetrating peptides (CPPs) can translocate across the plasma membrane of eukaryote cells and thus can be used for the intracellular delivery of biological cargo such as proteins and oligonucleotides.⁹⁻¹¹ Some CPPs internalize via endocytosis, but others use non-endocytosis pathways. In both cases, CPPs must translocate across the lipid membrane to enter a cell.

To date, most studies of the interactions of these peptides/proteins with lipid membranes have been done using a suspension of many small vesicles, such as large unilamellar vesicles (LUVs) with a diameter of 100–500 nm (the LUV suspension method). In these studies, the average values of the physical parameters of the vesicles are obtained from a large number of vesicles in different stages of the structural change or reaction induced by the peptide/protein. Consequently, much information has been lost.¹² For example, measurement of the membrane permeation (or leakage) of the internal contents of LUVs has been extensively used to investigate liposome interaction with various substances, including drugs, antibacterial substances, AMPs, PFTs, CPPs,

and fusogens.¹³⁻²³ However, the LUV suspension method does not allow determination of the main cause of membrane permeation because of a large number of factors potentially involved.¹² PFTs have also been investigated by analyzing their induced hemolysis of red blood cells (RBCs).^{18, 19} Many processes induce leakage of hemoglobin from the inside of RBCs (i.e., hemolysis); using this approach, the average leakage from many RBCs in a suspension is measured, similar to the LUV suspension method. The results obtained using the LUV suspension method and the hemolysis have provided the basis for many models and theories for the elementary processes and mechanisms of various reactions occurring in biomembranes, such as peptide/protein-induced pore formation. However, these models and theories have been proposed without experimental evidence of the elementary processes.

Giant unilamellar vesicles (GUVs) of lipid membranes with diameters greater than 10 μm have been used to investigate the physical and biological properties of vesicle membranes such as elasticity and shape change.²⁴⁻²⁹ Shape changes of a single GUV induced by compounds such as peptides, proteins, and small molecules can be measured in real time.²⁵⁻²⁹ Based on the characteristics of these GUVs, we have developed the single GUV method to investigate the functions and dynamics of biomembranes.^{12, 30-38} In this method, changes in the structure and physical properties of a single GUV that are induced by interactions of compounds such as peptides/proteins with the lipid membrane are observed as a function of time and spatial coordinates. The same experiment is repeated many times using other single GUVs. The results are used to analyze statistically the changes in the physical properties of a single GUV to obtain rate constants for the elementary processes underlying the structural changes and functions of GUVs (Fig. 1). This single GUV method can reveal details of the elementary processes of individual events, and allow calculation of their kinetic constants.

In this perspective, we describe the information on the interaction of AMP, PFT, and CPP with lipid membranes revealed by the single GUV method. In particular, we focus on the elementary processes of peptide/protein-induced pore formation in lipid membranes and the entry of peptides into single GUVs. Magainin 2 was used as a representative AMP, lysenin as a PFT, and transportan 10 (TP10) as a CPP. Lysenin is a 33.4 kDa PFT secreted by earthworms (*Eisenia foetida*) which specifically binds sphingomyelin (SM).^{18, 19, 39} Several experimental data indicate that lysenin molecules form oligomers in lipid membranes that contain SM. Transmission electron microscope images obtained using negative staining show that lysenin molecules form a hexagonal pattern in SM-containing membranes. The unit structure of this hexagon has a

diameter of 11 nm, which corresponds to that of a lysenin oligomer.^{19,39,40} On the other hand, TP, a synthetic CPP, consists of a neuropeptide, galanin, at the N-terminus and a wasp venom peptide, mastoparan, at the C-terminus. TP can translocate across the plasma membrane of cells by a receptor-independent mechanism.^{41,42} To reduce the inhibitory effect of TP on GTPase activity, a truncated analogue, TP10, has been synthesized by the deletion of six amino acids from the N-terminus of TP. TP10 also exhibits cell-penetrating activity.^{43,44} TP and TP10 can deliver a large protein such as an antibody, or an oligonucleotide or colloidal gold (diameter 10 nm) as cargo.^{42,44} Based on these results, we discuss the advantages of the single GUV method for revealing peptide/protein-induced pore formation processes in lipid membranes and the entry of peptides into vesicles.

2. Experimental procedures for the single GUV method

The detailed experimental procedure for the single GUV method was described in our previous review.¹² Here we only demonstrate several important points. GUVs of various lipid membranes are prepared in a buffer by the natural swelling of a dry lipid film using pre-hydration (i.e., the natural swelling method).^{27,32} There are many methods for preparing GUVs,⁴⁵ so the most suitable method for the specific purpose must be selected. If GUVs are to be used as large vessels for biochemical reactions, e.g., as artificial cells, the w/o emulsion method⁴⁶ is suitable because the efficiency of formation of unilamellar vesicles is relatively high. However, the disadvantage of the w/o emulsion method is that the GUV membrane contains oil. The presence of oils such as alkane inside the lipid membrane changes the physical properties of the lipid membrane, such as phase stability and structure, which affects the functions and structure of membrane proteins. Therefore, when GUVs are to be used to investigate the physical properties and interactions of compounds such as peptides/proteins with lipid membranes, the natural swelling method is the most suitable because the GUV membrane is oil-free and undamaged. The natural swelling method is thus used for the single GUV method. To prepare GUVs in a buffer with physiological ionic strength, intermembrane repulsion is necessary. For this purpose, we include negatively-charged lipids or poly-(ethylene glycol)[PEG]-grafted lipids in electrically neutral lipid membranes.⁴⁷ GUVs containing various water-soluble fluorescent probes were separated from free fluorescent probes using gel filtration chromatography³² or the membrane filtering method.⁴⁸ The latter method can also be used to prepare a large population of similar-sized GUVs composed of oil-free membranes, to purify GUVs

from smaller GUVs, LUVs, and various water-soluble compounds such as proteins and fluorescent probes, and to concentrate dilute GUV suspensions.⁴⁸

The purified GUV suspension is transferred to a chamber.¹² The GUVs settle on a cover slip or a microscope slide coated with bovine serum albumin (BSA)¹² or are connected to a cover slip or a microscope slide via a tether using the streptavidin-biotin system.³⁸ Suitable GUVs are visually selected using phase-contrast microscopy and are used for the single GUV method. A peptide/protein solution is continuously added to the vicinity of a single GUV through a micropipette during the interaction of peptide/protein with the GUV. Consequently, the equilibrium peptide/protein concentration near the GUV remains constant during the interaction, which is essentially the same as that in the micropipette.^{31, 35} During the interaction of peptide/protein with the single GUV, the structure of the GUV and the fluorescence intensity of the GUV are observed in real time using a phase-contrast fluorescence microscope equipped with a highly-sensitive EM-CCD camera, or with a confocal laser scanning microscope (CLSM).

2. Interaction of AMP magainin 2 with lipid membranes

2.1. Rate constants of magainin 2-induced pore formation in lipid membranes

Magainin 2 is a positively-charged peptide composed of 23 amino acids (GIGKFLHSAKKFGKAFVGEIMNS) with an amide-blocked C terminus. Magainin 2 can bind selectively to the negatively-charged outer monolayer of the bacterial cytoplasmic membrane due to electrostatic attraction.¹ Magainin 2 forms an α -helix in the lipid membrane interface, parallel to the membrane surface.^{49, 50}

The interaction of magainin 2 with lipid membranes has previously been investigated using the LUV suspension method.¹⁴⁻¹⁷ The most typical experiments to study the interaction of compounds with LUVs is the so-called leakage experiment, which monitors the compound-induced total average leakage of the internal contents of all the LUVs in the suspension as a function of time.^{12, 15-17} A large amount of leakage indicates that the compound strongly interacts with the lipid membrane, inducing instability in the structures of vesicles and lipid membranes. In a standard experiment, at the beginning each LUV contains a high concentration of a fluorescent probe and the fluorescence intensity is very low due to quenching of the fluorescence. After leakage of the fluorescent probe from the inside to the outside of the LUV, the fluorescence intensity increases because of the dilution of the probe outside the LUV. Several studies indicate that magainin 2 induces leakage of water-

soluble fluorescent probes (e.g., calcein) from LUVs of lipid membranes containing high concentrations of negatively-charged lipids such as PG. Magainin 2-induced leakage increases gradually over a 10 to 20 min period, and rate of leakage increases with higher concentrations of magainin 2. It is generally accepted that the main reason for the leakage is pore formation in the lipid membrane. However, many factors can induce leakage of water-soluble probes from the inside of LUVs: local disruption of the membrane due to membrane fusion and vesicle fission, instability of the membrane structure due to significant deformation of the vesicles, and the rupture of the vesicles. It is difficult to determine the exact cause of the leakage based on leakage experiments using the LUV suspension method because we cannot observe what happens in each vesicle when leakage occurs. Compound-induced leakage is due to several elementary processes such as pore formation in the lipid membrane, and the diffusion of the internal contents from the inside to the outside of the LUV through the pore. It is difficult to observe these elementary processes separately using the LUV suspension method.

Matsuzaki et al. observed the flip-flop of lipid molecules in magainin 2-induced leakage using the LUV suspension method.⁵¹ The rate of magainin 2-induced flip-flop does not depend on the type of lipid and it is similar to the rate of leakage. These results suggest that magainin 2-induced flip-flop occurs through a special structure such as a toroidal pore, where the outer and inner monolayers bend and merge in a toroidal fashion to create a pore in which the inner wall is composed of α -helical peptides and lipid head groups.^{52, 53} The chemical reaction of dithionite and a fluorescent probe (7-nitrobenz-2-oxa-1,3-diazoyl-4-yl, NBD) is used to measure the rate of flip-flop. Dithionite is small enough to pass through the magainin 2-induced pore easily and react with NBD attached to the lipid molecule in the inner monolayer. A decrease in fluorescence intensity after the fluorescent probe begins to leak does not indicate the flip-flop of lipids. To obtain clear information regarding the flip-flop of lipids, we must reveal the relationship between the leakage of the fluorescent probe and the decrease in fluorescence intensity of NBD-lipid with higher time resolution. In the suspension, each LUV is in a different stage of the reaction (i.e., all the elementary processes do not occur simultaneously). The LUV suspension method provides an average of the physical properties such as fluorescence intensity among these LUVs in different stages of the reaction. It is therefore difficult to elucidate the detailed relationship of the two events with higher time resolution.

In the LUV suspension method, the mode of leakage (or membrane permeation) of the fluorescent probes is classified as “all-or-none (i.e., in some LUVs all their fluorescent probes leak while in other LUVs no leakage

occurs)” or “graded (i.e., in all the LUVs their internal fluorescent probes leak gradually)”.⁵⁴⁻⁵⁶ Gregory et al. investigated magainin 2-induced leakage from 50% 1-oleoyl- 2-palmitoyl-phosphatidylglycerol(POPG)/50%1-oleoyl-2-palmitoyl-phosphatidylcholine(POPC)-LUVs and 30%POPG/70%POPC-LUVs using the ANTS/DPX assay, and found that magainin 2 induces all-or-none leakage.⁵⁵ This method provides unique information on the mode of compound-induced leakage, but the information on the elementary processes is qualitative: “all-or-none” leakage indicates that the rate of leakage of the internal contents is larger than that of compound-induced pore formation. In summary, the LUV suspension method provides information on magainin 2-induced leakage, but the elementary processes of the leakage and the mechanistic details of the interactions remain unclear.

In contrast, if we use the single GUV method, we can observe the interaction of magainin 2 with a single GUV and its induced leakage of a fluorescent probe from the inside of the single GUV as a function of time using fluorescence microscopy.^{32,33,36} Fig. 2 shows a typical experimental result of the interaction of magainin 2 with single GUVs composed of a mixture of negatively-charged dioleoylphosphatidylglycerol (DOPG) and electrically-neutral dioleoylphosphatidylcholine (DOPC) and containing a fluorescent dye, calcein, in the interior aqueous solution. The leakage of calcein occurs without local disruption, rupture of the GUVs, changes in local curvature of the membrane, membrane fusion and vesicle fission, indicating that magainin 2 forms pores in the membrane through which the membrane permeation of calcein occurs. The time course of the fluorescence intensity change of a single GUV provides two important pieces of information: one is the time required for pores to form in the membrane (i.e., the time at which the fluorescence intensity starts to decrease) and the other is the rate constant of membrane permeation of the fluorescent probe (based on the time course of the decrease in fluorescence intensity after pore formation) (Fig. 2B). Repetition of the same experiment many times using other single GUVs showed that the membrane permeation of calcein from the single GUVs starts stochastically (Fig. 2C), indicating that pores are formed stochastically in the lipid membrane. Membrane permeation in each GUV is complete within ~30 s after the start of membrane permeation (Fig. 2C). These results indicate that pore formation, rather than membrane permeation through the pore, is the rate-determining step. This agrees with the “all-or-none” mode of leakage, consistent with the results of the LUV suspension method.⁵⁵

Magainin 2-induced pore formation is likely an irreversible two-state transition: from magainin 2 binding to the outer monolayer of a GUV (i.e., the binding state), in which the membrane does not have any pores, to the state in which the GUV has pores (i.e., the pore state) (Fig. 2D). To determine the rate constant of the two-

state transition, k_p , from experimental results, we calculate the fraction of intact GUVs which do not have pores (i.e., where no membrane permeation of fluorescent probes occurs), $P_{\text{intact}}(t)$, among the population of GUVs examined. Analysis of the time course of $P_{\text{intact}}(t)$ provides the value of k_p . This rate constant is defined as the rate constant of peptide-induced pore formation in lipid membranes.^{32, 35} The time course of $P_{\text{intact}}(t)$ can be obtained from the above experimental results. Fig. 2E shows that $P_{\text{intact}}(t)$ of 60%DOPG/40%DOPC-GUVs decreased with time for each magainin 2 concentration. All the curves of the time course of $P_{\text{intact}}(t)$ in the presence of various concentrations of magainin 2 were well fit by a single exponential decay function defined by eq. (1) as follows,

$$P_{\text{intact}}(t) = \exp\{-k_p(t - t_{\text{eq}})\} \quad (1)$$

where t_{eq} is a fitting parameter and implies the time required for the binding equilibrium of magainin 2 from aqueous solution to the membrane interface of the GUV. The rate constant increased with increasing magainin 2 concentration: the average value of k_p for 5 μM magainin 2 ($(5.3 \pm 1.1) \times 10^{-2} \text{ s}^{-1}$) was about 30 times larger than that of k_p for 2 μM magainin 2 ($(1.7 \pm 0.7) \times 10^{-3} \text{ s}^{-1}$) (Fig. 3A).

One of the main factors that mediate the binding of magainin 2 to lipid membranes is the electrostatic attraction between the positively-charged magainin 2 and the negatively-charged lipid membranes. k_p greatly depends on the DOPG concentration in the GUV membrane (i.e., the surface charge density of the membrane (Fig. 3A)). The magainin 2 concentration in the buffer required to induce the same value of k_p increases significantly with decreasing DOPG concentrations (i.e., with decreasing surface charge density of the membrane). k_p also depends on the salt concentration: it increases with a decrease in NaCl concentration.³⁵ It is well known that electrostatic interactions due to the surface charges of lipid membranes increase with increasing surface charge density or with decreasing salt concentration.⁵⁷⁻⁶⁰ These results clearly indicate that k_p increases with an increase in electrostatic interactions due to the surface charges of lipid membranes. Using the Poisson-Boltzmann equation and the experimentally determined intrinsic binding constants of magainin 2 to lipid membrane, we can convert the magainin 2 concentration in the buffer to the magainin 2 concentration at the membrane interface (or the surface concentration of magainin 2), which is expressed by the molar ratio of magainin 2 bound to the membrane interface to lipid in the outer monolayer of a GUV, X (mol/mol). Fig. 3B shows the dependence of k_p on X . This dependence was obtained by replotting the graphs of the dependence of k_p on magainin 2 concentrations in the buffer (Fig. 3A). The dependences of k_p on X for 40%DOPG/60%DOPC-

and 30%DOPG/70%DOPC-GUVs in buffer A are almost the same (i.e., the two curves almost superimpose). Magainin 2-induced pore formation occurs at and above $X = 70$ mmol/mol, and both the k_p values increased with an increase in X . The results clearly indicate that X determines the rate constant of magainin 2-induced pore formation.

2.2. Rate constants of membrane permeation (or leakage) of fluorescence probes of various sizes through magainin 2-induced pores in lipid membranes

The rate constant of membrane permeation (or leakage) of fluorescent probes through pores in the GUV membrane induced by compounds such as peptides/proteins (Fig. 4A) is a good measure for evaluating the size and number of pores and also the time course of the change in size and number of pores. The rate constant of membrane permeation cannot be measured using the LUV suspension method because this method can provide only the total amount of leakage from all the LUVs in the suspension. However, using the single GUV method, we can determine this rate constant by analyzing the time course of fluorescence intensity change of a GUV after pore formation. Generally, the rate constant of membrane permeation of the fluorescent probe through a GUV membrane, k_{mp} , is determined by the number and size of the pores. Analysis of the time course of k_{mp} can therefore provide information on the temporal change in pore size and the number of pores. Fig. 4B shows the time course of the change in the normalized fluorescence intensity of several “single GUVs” containing Texas-Red dextran 10,000 (TRD-10k) (Stokes-Einstein radius, R_{SE} , is 2.7 nm) induced by 7 μ M magainin 2. Rapid leakage of TRD-10k was observed from each single GUV that started in a stochastic manner, then the rate of membrane permeation decreased and the resulting slower membrane permeation continued. When 4 μ M magainin 2 was used (Fig. 4C), this characteristic of membrane permeation was more clearly observed. Similar characteristics were observed for magainin 2-induced membrane permeation of Texas-Red dextran 3,000 (TRD-3k) ($R_{SE} = 1.4$ nm) and Alexa-Fluor trypsin inhibitor ($R_{SE} = 2.8$ nm): a transient rapid membrane permeation during the initial stage, followed by a stage of slow membrane permeation. In contrast, magainin 2 induced only a transient, but very small (10-20%) membrane permeation of larger fluorescent probes such as Texas-Red dextran 40,000 (TRD-40k) ($R_{SE} = 5.0$ nm) and FITC-BSA ($R_{SE} = 3.6$ nm) (Table 1).

The rate constant of the membrane permeation of the fluorescent probe from a GUV, k_{mp} , is determined by the following formula,

$$FI(t) = I(t) / I(0) = \exp(-k_{mp}(t)t) \quad (2)$$

where $I(t)$ and $I(0)$ are the fluorescence intensity of the inside of the GUV at time t after, and before, initiation of membrane permeation, respectively, and $FI(t) (= I(t)/I(0))$ is the normalized fluorescence intensity. If we plot the log of FI vs. time (s), the rate constant of membrane permeation, $k_{mp}(t)$, can be obtained from the slope of the curve quantitatively (Fig. 4D). Generally $k_{mp}(t)$ changes with time. In the magainin 2-induced pore, there are two linear regions in this curve (Fig. 4D), which provide two k_{mp} rate constants: k_{mp}^{initial} of the rapid membrane permeation at the initial stage and k_{mp}^{steady} of the slow membrane permeation at the final steady stage. For each probe, the value of k_{mp}^{initial} is 20–40 times greater than that of k_{mp}^{steady} under the same experimental conditions (Table 1). These results indicate that magainin 2 molecules initially induce a large, transient pore in lipid membranes, then the radius of the pore decreases to a stable smaller size. Since membrane permeation of AF-SBTI did not occur at the final stage for 7 (or 4) μM magainin 2, we conclude that the radius of the pore induced by 7 (or 4) μM magainin 2 at the final stage is smaller than 2.8 nm (R_{SE} of SBTI), but is larger than 1.4 nm (R_{SE} of TRD-3k). This value agrees with that of magainin 2-induced pores in multilayer membranes determined by neutron in-plane scattering (1.9 nm).⁶¹ On the other hand, 15 μM magainin 2 induced the membrane permeation of AF-SBTI, but not BSA, indicating that the radius of the pores at the final stage induced by 15 μM magainin 2 is larger than 2.8 nm but smaller than 3.6 nm (R_{SE} of BSA), which is larger than that induced by 7 (or 4) μM magainin 2. These results clearly indicate that the radius of the magainin 2-induced pore at the final stage increases with an increase in magainin 2 concentration. Theoretical analysis of the rate constant of membrane permeation at the initial stage provided values for the radius of the pore. This radius at the initial stage increased with magainin 2 concentration and also increased with the radius of the GUV.³⁶ These data provide the first information concerning the kinetic pathway of peptide/protein-induced pore formation in lipid membranes. Based on these data, we proposed a hypothesis regarding the mechanism of magainin 2-induced pore formation.³⁶

Subsequently, other examples of the change in the size of peptide/protein-induced pores were found using the GUV suspension method.^{62, 63} In this method, many GUVs are suspended in a solution of water-soluble fluorescent probes and peptides/proteins, and the changes in the physical properties of single GUVs are observed. Fuertes et al. investigated pore formation in lipid membranes induced by the $\alpha 5$ segment of the proapoptotic protein, Bax (Bax $\alpha 5$).⁶² When GUVs are suspended in a solution of two fluorescent probes, Alexa555 (1.25

kDa) and calcein-labeled dextran 10,000 (FD10; 10 kDa) ($R_{SE} = 2.3$ nm), both fluorescent probes enter the GUV at a similar rate initially, but later the rate of entry of FD10 becomes smaller than that of Alexa555. This result indicates that the size of this pore is large at the initial stage, and then decreases and equilibrates to a smaller pore. These findings are similar to the phenomena observed with magainin 2-induced pore formation. Bleicken et al. indicated that proapoptotic proteins, Bax and Bak Δ C21 (Bak lacking the carboxyl-terminal 21 amino acids), form pores through which cytochrome C (12 kDa) and allophycocyanine (104 kDa) can pass, and also that the size of these pores changes with time and depends on the protein concentration.⁶³ Therefore, we can conclude that the single GUV method and the GUV suspension method are useful techniques for following the evolution (such as the size change) of peptide/protein-induced pores in lipid membranes. At present, no other method can provide this information.

3. PFT lysenin-induced pore formation in lipid membranes

Lysenin is a PFT that can bind specifically to SM.¹⁸ The binding constant of lysenin to SM, determined by surface plasmon resonance experiments, is large: the dissociation constant of lysenin to 100% SM membrane is 5.3 nM.¹⁸ The molecular weight of lysenin is 33 kDa. Lysenin exists as a monomer in buffer. If lysenin binds to lipid membranes containing SM, it forms SDS-resistant oligomers which can be detected using SDS-PAGE. The so-called pore-forming activity of lysenin has been investigated by leakage of a fluorescent probe from LUVs using the LUV suspension method, and by analysis of its induced hemolysis of RBCs (i.e., the leakage of hemoglobin from the inside of RBCs).¹⁸⁻²⁰ Lysenin-induced leakage of calcein from LUVs of lipid membranes containing SM increases gradually over a 10 to 60 min period, and the rate of leakage increases with an increase in lysenin concentration and temperature.¹⁸ Lysenin cannot induce leakage from LUVs containing other sphingolipids such as ceramide and sphingosine, indicating that the specificity of the binding of lysenin to SM is very high.¹⁸ Lysenin-induced hemolysis increases with an increase in lysenin concentration, which has significant temperature dependence; for example, hemolysis activity at 37 °C is much larger than that at 4 °C.¹⁹ The hemolysis assay is a popular methodology for checking the activity of PFTs. However, it is difficult to identify the main factor underlying hemolysis.³⁷ For example, membrane fusion by viruses induces hemolysis.⁵⁶ The rupture and fragmentation of RBCs also cause hemolysis. Therefore, we can conclude that the hemolysis activity of peptides/proteins indicates that they interact with RBC membranes strongly and perturb them. Yamaji et al. found that the coexistence of small unilamellar vesicles (SUVs) containing SM in a suspension of RBCs

inhibits lysenin-induced hemolysis. SM/cholesterol (chol)-SUVs are 10,000 times more effective in inhibiting hemolysis than SM-SUVs.¹⁸ Ishitsuka et al. found that the binding constant of lysenin to SM in SM/chol membranes is similar to that for SM membrane, but the presence of cholesterol increases the fraction of oligomers.⁴⁰ Therefore, one of the main factors for the higher efficiency of the inhibition of hemolysis by SM/chol-SUVs is the increase in the fraction of lysenin oligomers in the membrane.²¹

In contrast with the LUV suspension method and the hemolysis method, if we use the single GUV method, we can observe the interaction of lysenin with a single GUV and its induced leakage of a fluorescent probe from the inside of the single GUV as a function of time using fluorescence microscopy.³⁷ Fig. 5 shows a typical experimental result of the interaction of lysenin with DOPC/SM/cholesterol (chol) (42/30/28)-GUVs containing calcein. The results clearly show that lysenin molecules form pores in the DOPC/SM/chol membrane, through which membrane permeation of calcein occurs without disruption of the GUVs (Fig. 5A). As described above, the rate constant of the membrane permeation of the probe $k_{mp}(t)$ is determined by analysis of the time course of $FI (= I(t)/I(0))$. The value of $k_{mp}(t)$ first increased over time, and then remained constant after achieving a maximum value at 170 s. This maximum value did not change for up to 450 s. It is note that values of $k_{mp}(t)$ depend on the size or the radius of a GUV, and hence to compare these values we must use GUVs of similar size. However, it is sometimes difficult to prepare similar sized GUVs composed of different lipid compositions. In contrast, the membrane permeability coefficient, $P(t) (= r k_{mp}(t)/3$, where r is the radius of a GUV), does not depend on the size of GUVs.³⁷ If we use $P(t)$, we can explain the results shown in Fig. 5B as follows: after pore formation, the value of P increased with time and then reached a steady, maximum value, P^s , which remained constant for a long time (280 s). The P^s value for Fig. 5B was obtained ($P^s = 2.0 \times 10^{-2} \mu\text{m/s}$). The dependence of P^s on lysenin concentration, C , in Fig. 5C shows that P^s increases with C . The average value of P^s for 600 ng/mL lysenin ($(1.5 \pm 0.2) \times 10^{-1} \mu\text{m/s}$) is approximately 20 times larger than the P^s value for 10 ng/mL lysenin ($(6.9 \pm 1.7) \times 10^{-3} \mu\text{m/s}$). In contrast, the interaction of 600 ng/mL lysenin with single SM/DOPC/chol (42/30/28)-GUVs containing AF-SBTI did not induce a change in the fluorescence intensity of the inside of the GUV, indicating that membrane permeation of AF-SBTI through lysenin-induced pores did not occur. Based on these results, we conclude that the radius of the lysenin-induced pore is smaller than 2.8 nm (the R_{SE} of SBTI) but larger than 0.74 nm (the R_{SE} of calcein).

Generally, the P^s value depends on the size of the pore and the number of pores per unit area of a membrane. If we consider that lysenin molecules form pores all with the same diameter, the value of $P(t)$ of the lipid membrane is determined by the permeability coefficient of a single pore (P_1), the fraction of pores in the open state or their probability of opening (P_{open}), and the pore concentration or the number of pores per unit area ($N_p(t)$). Thus, the equation $P(t)$ is $P(t) = P_1 P_{\text{open}} N_p(t)$. We can therefore interpret the result of Fig. 5B as follows. A pore is first formed in the lipid membrane, following which N_p increases over time and finally reaches a steady, maximum value, N_p^s .

It is important to elucidate the effect of cholesterol on lysenin-induced membrane permeation. The data in Fig. 5C show that the lysenin concentration dependence of P^s of membranes without cholesterol (SM/DOPC (58/42)-GUVs) is much greater than that of membranes with cholesterol (SM/DOPC/chol (42/30/28)). Thus, at low concentrations of lysenin, the P^s values of membranes containing cholesterol (SM/DOPC/chol (42/30/28)) are much larger than those of membranes without cholesterol (SM/DOPC (58/42)-GUVs). This indicates that the presence of cholesterol increases the P^s value (and thereby the N_p^s value) at low concentrations of lysenin. The fraction of lysenin present as an SDS-resistant oligomer (i.e., the SDS-resistant oligomer fraction of lysenin) increases as the SM/lysenin molar ratio decreases, and its dependence on the SM/lysenin ratio is much greater in the absence of cholesterol (SM/DOPC (58/42)-SUVs) than in the presence of cholesterol (SM/DOPC/chol (42/30/28)) (Fig. 5E). Thus, at low concentrations of lysenin, the oligomer fractions of lysenin in membranes containing cholesterol (SM/DOPC/chol (42/30/28)) are much larger than those in membranes without cholesterol (SM/DOPC (58/42)-GUVs). These results show a strong correlation between the lysenin-induced membrane permeability coefficient and the SDS-resistant oligomerization of lysenin in SM/DOPC (58/42) and SM/DOPC/chol (42/30/28) membranes, indicating that the pore concentration increases with an increase in the oligomer fraction. The presence of cholesterol induces phase separation between the liquid-ordered (*lo*)-phase domain (in Fig. 5F, the domains with low fluorescence intensity) and the liquid-disordered (*ld*) phase domain (in Fig. 5F, the domains with high fluorescence intensity) in SM/DOPC/chol membranes. The diffusion coefficient in the *lo* phase is relatively large, which is one of the main reasons why the presence of cholesterol increases the oligomer fraction and the pore concentration.

Using the single GUV method, it is also possible to estimate the rate constant of lysenin-induced pore formation. Several possible schemes for lysenin-induced pore formation could be involved in generating the

intermediate states (i.e., the oligomer states); currently, we cannot identify the correct scheme due to limited experimental data.³⁷ If the rate of oligomerization of lysenin in the membrane is much larger than that of the conversion from the oligomer to the pore, i.e., if the rate-determining step is the conversion from the oligomer to the pore, we can apply the irreversible two-state transition model and obtain values of k_p which correspond to the rate constants of the transition from the oligomer state to the pore state. In other cases, k_p has a different physical meaning. Time courses of P_{intact} of SM/DOPC/chol (42/30/28)-GUVs in the presence of various concentrations of lysenin can be fit by a single exponential decay function defined by eq. (1). The rate constant of pore formation increases with increasing lysenin concentration: the average k_p of 600 ng/mL lysenin ($(2.6 \pm 0.1) \times 10^{-1} \text{ s}^{-1}$) is ~ 70 times larger than that of k_p for 10 ng/mL lysenin ($(3.6 \pm 0.1) \times 10^{-3} \text{ s}^{-1}$) (Fig. 6E). This result suggests that the rate of oligomerization of lysenin in the membrane is high and that the rate determining step is the oligomer-induced pore formation. For the SM/DOPC/chol (42/30/28) membrane, lysenin molecules bound to SM molecules in a SM/chol-rich domain in the *l_o*-phase can rapidly diffuse within this domain and frequently collide with other lysenin molecules bound to SM molecules, resulting in a high rate of lysenin oligomerization. In contrast, in the case of SM/DOPC (58/42)-GUVs, time courses of P_{intact} cannot be fit well by a single exponential function. In this case, lysenin molecules bound to SM molecules in a SM-rich domain, which is similar to a gel phase, cannot diffuse rapidly, and therefore the oligomerization step becomes the rate-determining step.

Lysenin can form pores in GUVs of SM/chol (60/40) membrane in homogeneous *l_o* phase, indicating that the phase boundary between the *l_o* and the *l_d* phases is not necessary for lysenin-induced pore formation (Fig. 6A, B). However, the P^s values of SM/chol (60/40)-GUVs are smaller than those of SM/DOPC/chol (42/30/28)-GUVs (Fig. 6C), even though the SDS-resistant oligomer fractions are similar for both membranes (Fig. 6D). This suggests that not all of the oligomers can convert into a pore. Time courses of P_{intact} of SM/chol (60/40)-GUVs in the presence of various concentrations of lysenin can be fit approximately by a single exponential decay function defined by eq. (1). The k_p values of SM/chol (60/40)-GUVs are much smaller than those of SM/DOPC/chol (42/30/28)-GUV, irrespective of lysenin concentration (Fig. 6E). These results for the rate constant are consistent with the above interpretations regarding the P^s values.

Recently, the ion channel activity of a lysenin-induced pore in a planar membrane was measured using single channel recording measurements.⁶⁴ The single channel conductance of a lysenin-induced pore for NaCl is

540 pS. No closing events were observed for the pore, indicating that $P_{\text{open}} = 1$. The single GUV method currently cannot provide information on the permeability coefficient of a single pore, P_1 , and therefore the single channel recording method is superior in this regard. However, it is difficult to obtain information on the state of the membrane before pore formation (i.e., the kinetics of initial pore formation) and on the rapid change in pore size using single channel recording. This is discussed in detail below.

Using the GUV suspension method, Schön et al. investigated the interaction of equinatoxin, a PFT, with GUVs.⁶⁵ In the presence of equinatoxin, Alexa Fluor 488 (AF488) enters the GUV interior from the outside bulk solution, indicating that equinatoxin induces membrane permeation of AF488. The volume flux (similar to the membrane permeability coefficient, $P(t)$) of AF488 does not change with time. Their data suggest that equinatoxin forms pores only when the l_o and the l_d phases coexist, indicating that the phase boundary between these two phases plays an important role in equinatoxin-induced pore formation. These results are different from those of lysenin described above.

4. Entry of CPP transportan 10 (TP10) into a single vesicle by translocating across the lipid membrane

The entry of CPPs and their cargo delivery into cells are observed using fluorescence microscopy and electron microscopy.⁹⁻¹¹ The mechanism by which CPPs and their cargo translocate across the plasma membrane is still controversial. Some CPPs internalize via endocytosis, but others use non-endocytosis pathways. In both cases, CPPs must translocate across the lipid bilayer to enter a cell. To reveal the mechanism of translocation, it is important to elucidate the interaction of CPPs with lipid membranes. Various experiments have been conducted using the LUV suspension method to determine binding constants and leakage of the internal contents.²¹⁻²³ The translocation of peptides from the outer monolayer to the vesicle interior has been studied using energy transfer from the tryptophan of magainin 2 to dansyl-labelled lipids in the membrane. The results indicate that some fractions of magainin 2 translocate into the inside of LUVs.¹⁴ For example, when trypsin (a protease) is added to a suspension of magainin 2 and LUVs of lipid membrane containing dansyl-labelled lipids, a short segment of magainin 2 in the outer monolayer is digested and desorbs from the membrane surface, resulting in a decrease in energy transfer and the fluorescence intensity of dansyl-lipid excited at 280 nm becomes zero. As the interaction time between magainin 2 and the LUVs increases, the addition of trypsin does not decrease the fluorescence intensity to zero, and the remaining fluorescence intensity increases, indicating

that magainin 2 enters the LUVs at trypsin-free areas.¹⁴ The time course of magainin 2-induced leakage of fluorescent probes is similar to that of translocation.¹⁴ These results suggest that the translocation of magainin 2 into the LUVs occurs after pore formation in the membrane. However, using the LUV suspension method, it is difficult to reveal the relationship between the leakage of fluorescence probe and the translocation of peptides with higher time resolution.

TP10 is a positively-charged peptide composed of 21 amino acids (AGYLLGKINLKALAALAKKIL) with an amide-blocked C terminus. The interaction of TP10 with lipid membranes has been investigated using the LUV suspension method.²¹⁻²³ TP10 induces gradual leakage (membrane permeation) of a small water-soluble fluorescent probe, carboxyfluorescein, from the inside to the outside of LUVs. The rate of leakage increases with an increase in TP10 concentration in the buffer.²¹ The rate constants for LUV membrane binding and dissociation of TP10 were determined. Yandek et al. found that the TP10-induced leakage of fluorescent probes is “graded” based on the results of fluorescence ANTS/DPX assays.²¹ The kinetic scheme of the interaction of TP10 with the membranes, and of the entry of TP10 into a vesicle, were analyzed assuming that these fluorescent probes leak during the translocation of TP10 across the lipid bilayer.^{21, 23} This state was defined as the TP10-induced pore in the lipid membrane.

In contrast, if we use the single GUV method, we can observe the elementary processes for the entry of CPPs and obtain their kinetics. Fig. 7 shows a typical experimental result of the simultaneous measurement of the translocation of a fluorescent probe, carboxyfluorescein (CF)-labeled TP10 (CF-TP10), across the lipid membrane and the membrane permeation of a water-soluble fluorescein probe, Alexa Fluor 647 hydrazide (AF647), from 20%DOPG/79%DOPC/1%biotin-lipid-GUVs containing smaller vesicles composed of 20%DOPG/80%DOPC. The data were obtained using confocal laser scanning microscopy (CLSM). Fig. 7A (1) and B show that CF-TP10 induces pores in the GUV membrane at 210 s, then membrane permeation of AF647 occurs through the pores rapidly. On the other hand, Fig. 7A (2) shows that the fluorescence intensity of the GUV membrane gradually increases and is almost saturated at 100 s (green squares in Fig. 7B), indicating that the concentration of CF-TP10 in the GUV membrane gradually increases and at 100 s is almost saturated. Some fluctuations in the intensity of the GUV membrane are caused by the smaller vesicles inside the GUV near the GUV membrane. At the beginning of the interaction, there was no fluorescence inside the GUV, but after 140 s, fluorescence intensity was observed due to the membranes of the smaller vesicles inside the GUV

($t = 144, 167, \text{ and } 194 \text{ s}$ in Fig. 7A(2)). This fluorescence occurred before CF-TP10-induced pore formation (210 s). These results indicate that CF-TP10 enters the GUV from the outside by translocating across the GUV membrane and then binds to the membrane of the smaller vesicles inside the GUV. The entry of CF-TP10 into the GUV occurs before pore formation.

We can also obtain detailed information on the concentration dependence of the entry of CF-TP10 into a GUV before pore formation (i.e., before the membrane permeation of AF647) (Fig. 7C). At and above $0.6 \mu\text{M}$ CF-TP10, the entry of CF-TP10 is observed in some GUVs. The fraction of entry of CF-TP10 increases with an increase in CF-TP10 concentration and becomes 1.0 at and above $1.0 \mu\text{M}$. These results clearly indicate that the translocation of CF-TP10 is a necessary condition, but not a sufficient condition, for pore formation, i.e., some other factor determines pore formation. The rate constant of CF-TP10-induced pore formation, k_p , can be obtained by analyzing the time course of P_{intact} . Fig. 7D shows the dependence of the rate constant of CF-TP10 (or TP10)-induced pore formation on the concentration of CF-TP10 (or TP10). The rate constant increases with an increase in peptide concentration.

Data showing the time course of the fluorescence intensity of the rim of a GUV which does not contain smaller vesicles (green squares in Fig. 8A) indicate the time course of CF-TP10 concentration in the GUV membrane. The time derivatives of the CF-TP10 concentrations in the outer monolayer, the inner monolayer of the GUV, and in the aqueous solution inside the GUV, can be expressed by differential equations.³⁸ Generally it is difficult to obtain the average concentration of CF-TP10 in the GUV membrane, $C_M(t)$, due to several unknown parameters. However, if the transfer of CF-TP10 between the outer and the inner monolayers is fast, i.e., the rate of the transfer is higher than the rate constant of the binding of CF-TP10 to the GUV membrane and the rate constant of its dissociation from the membrane into aqueous solution, we can obtain $C_M(t)$ as follows,

38

$$C_M(t) = \frac{C_M^{\text{max}}}{1 + \frac{1}{2K_B C_{\text{out}}^{\text{eq}}}} \left[1 - \exp \left\{ - \left(\frac{1}{2} k_{\text{ON}} C_{\text{out}}^{\text{eq}} + k_{\text{OFF}} \right) t \right\} \right] \quad (3)$$

$$= A [1 - \exp(-k_{\text{app}} t)]$$

$$\text{where } k_{\text{app}} = k_{\text{ON}} C_{\text{out}}^{\text{eq}} / 2 + k_{\text{OFF}} \quad (4)$$

where k_{ON} is the rate constant of the binding (or association) of CF-TP10 to the GUV membrane, k_{OFF} is the rate constant of the dissociation of CF-TP10 from the membrane into the aqueous solution surrounding the GUV,

$C_{\text{out}}^{\text{eq}}$ is the CF-TP10 concentration in aqueous solution near the GUV, $K_B = k_{\text{ON}}/k_{\text{OFF}}$ is the binding constant of CF-TP10 to the membrane, and k_{app} is the apparent rate constant of the increase in $C_M(t)$. The time course of the fluorescence intensity of the rim of the GUV (Fig. 8A) can be fit well by eq. (3) (the black line in Fig. 8A), which gave a value for the rate constant k_{app} of 0.026 s^{-1} . Figure 8B shows that k_{app} increased linearly with an increase in $C_{\text{out}}^{\text{eq}}$. Fitting the data in Fig. 8B to eq. (4) provides values for k_{ON} and k_{OFF} : $k_{\text{ON}} = 2.2 \times 10^4 \text{ M}^{-1}\text{s}^{-1}$ and $k_{\text{OFF}} = 4.2 \times 10^{-3} \text{ s}^{-1}$ (i.e., $K_B = 5.2 \times 10^6 \text{ M}^{-1}$). Hence, using the single GUV method, we can obtain information on the time course of CF-TP10 concentration in the GUV membrane. Although several assumptions must be made, analysis of these data provides the rate constants of the association and dissociation of CF-TP10 with the GUV membrane.

On the other hand, the GUV suspension method has been applied to the interaction of CPPs with GUVs.⁶⁶⁻⁶⁸ Thorén et al. showed that fluorescent probe-labeled penetratin entered the GUVs composed of soybean phosphatidylcholine, although they could not measure the leakage of water-soluble fluorescent probe using these GUVs.⁶⁶ Mishra et al. investigated the interaction of fluorescent probe-labeled R6 and HIV TAT peptides with GUVs composed of DOPC/DOPS (dioleoylphosphatidylserine)/DOPE (dioleoylphosphatidylethanolamine) = 20/20/60 containing water-soluble fluorescent probes. They found that these fluorescent probe-labeled peptides induced leakage of the water-soluble fluorescent probes, then these peptides entered the GUVs.⁶⁷ However, as the time course of these processes could not be obtained, it was not possible to analyze the leakage and entry quantitatively. Recently, Wheaton et al. investigated the interaction of lissamine rhodamine B (Rh)-labeled CPPs (TP10W and DL1a) with GUVs containing smaller GUVs in a solution of a water-soluble fluorescent probe, carboxyfluorescein (CF).⁶⁸ First, CF and peptides entered the interior of the outer GUV, then the translocation of peptides and the influx of CF into the inner GUVs occurred. They observed that the translocation of peptide into the inner GUVs occurred gradually whereas the influx of CF into the inner GUVs occurred rapidly. However, they could not obtain quantitative results such as the peptide concentration dependence of the translocation of peptides and the rate constant of the peptide-induced pore formation.

5. Advantages of the single GUV method

There are several advantages of the single GUV method over the LUV suspension method and the hemolysis method. First, it is easy to identify the cause of the compound-induced membrane permeation (or leakage) of fluorescent probes inside a vesicle. Generally, many factors induce the leakage of the internal contents of liposomes, such as fluorescent probes, and the leakage of hemoglobin from RBCs (i.e., hemolysis). It is difficult to identify the main factor responsible for leakage (or membrane permeation) using the LUV suspension method and hemolysis.¹² For example, membrane fusion by viruses induces hemolysis,⁶⁹ and polyethylene glycol-induced membrane fusion induces leakage of the internal contents of liposomes.¹³ Rupture and fragmentation of liposomes or RBCs also cause leakage and hemolysis. These factors, such as membrane fusion and rupture, can be easily detected using the single GUV method.^{32,33} Therefore, the detection of leakage using the LUV suspension and hemolysis methods does not always indicate pore formation in lipid membranes.

Second, measurements using the single GUV method allow us to separate the compound-induced-pore formation step in lipid membranes from the membrane permeation of a fluorescent probe through the pores, allowing the rate constants of these elementary processes to be obtained. We determined the rate constants of pore formation induced by magainin 2, lysenin, and TP10. For magainin 2 and TP10, the binding of these peptides to the lipid membrane rapidly reached equilibrium, allowing us to reasonably consider the process as an irreversible two-state transition from the binding state (i.e., the binding state of magainin 2 in the outer monolayer, or the binding state of TP10 in the outer and the inner monolayers) to the pore state. Recently, the same analysis using the time course of P_{intact} of single GUVs provided the rate constant of external tension-induced pore formation in a GUV.⁷⁰ For lysenin, there is another elementary process between the binding of the protein to the lipid membrane and pore formation, namely, the formation of lysenin oligomer. Many schemes to explain PFT-induced pore formation have been proposed. For example, PFT molecules in a buffer bind to a lipid membrane, then a monomer of the bound PFT diffuses laterally in the membrane and collides with another monomer to form an oligomer and finally a conformational change in the oligomer induces pore formation.^{8,71} In some PFTs, monomeric PFT protein segments may insert into a membrane during binding and then they associate to form an oligomer (i.e., a pore), but in others, the insertion of protein segments occurs after the oligomer formation and then they form a pore. For lysenin-induced pore formation, several schemes can be proposed to describe the intermediate states (i.e., the oligomer state), but currently the correct scheme cannot be identified due to limited experimental data. Therefore, an interpretation of the rate constant of lysenin-

induced pore formation is required.³⁷ We have also determined the rate constant of membrane permeation, or the membrane permeability coefficient, of a fluorescent probe through these peptide/protein-induced pores. Analysis of this rate constant can provide information on the size of the pores, and on the change in the size and number of these pores over time.^{36, 37} In the LUV suspension method, the mode of leakage (or membrane permeation) of fluorescent probes is classified as “all-or-none” or “graded”.⁵⁴⁻⁵⁶ In contrast, in the single GUV method, we use only rate constants of pore formation and rate constants of membrane permeation determined from single GUVs. Furthermore, it is important to elucidate the effects of mutation of proteins/peptides such as AMPs, PFTs, and CPPs on their pore formation in lipid membranes and membrane permeation through these pores, and the effects of lipid composition and the physical properties of lipid membranes on their pore formation and membrane permeation. Experimental data on the effects of mutation on the kinetic constants of pore formation and those of membrane permeation through the pore determined using the single GUV method could provide valuable information.

Third, using the single GUV method with a CLSM, we can observe and analyze the time course of the entry of CPPs into a single GUV, and the relationship between the entry of CPPs and its induced pore formation. An experiment designed to simultaneously observe membrane permeation of the fluorescent probe and the entry of CF-TP10 into a GUV clearly shows that CF-TP10 translocates across the lipid membrane before pore formation. The time course of the increase in peptide concentration in the GUV membrane can also be obtained using a CLSM. These results cannot be obtained using the LUV suspension method.

Next, we compare the single GUV method with the GUV suspension method. In the GUV suspension method, many GUVs are suspended in a solution of water-soluble fluorescent probes and peptides/proteins and changes in the physical properties of many GUVs are observed.^{62, 63, 65, 67, 68, 72-74} The advantages of the single GUV method over the GUV suspension method are as follows. (1) In the single GUV method, we can observe the change in the structure and physical properties, such as fluorescence intensity, of a single GUV from the start of the interaction of peptide/protein with the GUV (i.e., $t = 0$). This allows determination of the rate constant of pore formation. We can also follow rapid pore formation or rapid peptide translocation. In contrast, it is difficult to obtain rate constants of pore formation using the GUV suspension method because it is difficult to observe the start of the interaction of peptide/protein with the GUV. (2) In the single GUV method, we can control the concentration of peptide/protein outside a single GUV (i.e., $C_{\text{out}}^{\text{eq}}$), and therefore we can obtain

detailed information on the peptide/protein concentration dependence of peptide/protein-induced pore formation, membrane permeation through the pores, and the entry of peptides into a GUV. In contrast, in the GUV suspension method, many GUVs are added to a given concentration of peptide/protein solution, so the peptide/protein concentration outside the GUV depends on the GUV concentration (i.e., lipid concentration) in the suspension. Therefore, $C_{\text{out}}^{\text{eq}}$ cannot be controlled precisely, and it also changes with time because the binding of peptides/proteins with GUV membranes, and the entry of peptides into the GUVs, increases with time. The same drawbacks are observed with the LUV suspension method. Both suspension methods utilize the concept of “peptide (or protein) to lipid molar ratio in the total suspension, P/L ”, which is the average ratio in all the vesicles. The concentration of peptide/protein surrounding vesicles cannot be expressed by P/L , and therefore P/L cannot be used to describe reaction rate equations. The most important physical quantity that determines the various phenomena occurring in lipid membranes is the molar ratio of peptide (or protein) to lipid in a lipid membrane, i.e., the surface concentration of peptide (or protein), X . However, P/L is equal to X only if the binding constant of peptide (or protein) to the lipid membrane is so large that all the peptides (or proteins) bind to the membrane. On the other hand, an advantage of the GUV suspension method is that no special equipment and experimental technique, such as the handling of micropipettes, is required. It is evident that both the single GUV method and the GUV suspension method are superior to the LUV suspension method, and hence these powerful methods are increasingly revealing the mechanism of interaction of peptides/proteins with lipid membranes.

It is useful to compare the single GUV method with the single channel recording (SCR) of ion channel proteins and ion channel-forming peptides in a planar bilayer.^{64, 75-79} SCR is a very sensitive, accurate method for measuring the current passing through a single channel and obtaining the single channel conductance. Statistical analysis of the fluctuation of the current provides the life-time of the open state and the closed state of the single channels, and also some information on the interaction of compounds with the ion channel (e.g., flickering). In these points, SCR is superior to the single GUV method, because it is difficult to obtain information on the membrane permeability of ions through a single pore and on the dynamics of a single pore in lipid membranes using the single GUV method. In SCR, after forming a single ion channel in the stable planar membrane, it is possible to measure the current through the channel reproducibly. However, in most cases it is not easy to obtain reproducible data on the change in current before a single channel is formed in the membrane.

For example, when peptides are added to the preformed planar membranes, large irregular and non-reproducible fluctuations in the current are often observed, but after a single channel is formed in the membrane, a steady single channel current is observed. On the other hand, the single GUV method enables us to observe and measure the state of membranes before pore formation reproducibly, which provides information on the elementary processes underlying the interaction of peptide/protein with lipid membranes at the initial steps. In SCR measurements, it is difficult, but not impossible, to measure irreversible pore formation because it is much easier to analyze SCR data of the reversible transition between the open and closed states of single channels quantitatively. Moreover, the rapid change in the pore size, corresponding to the rapid change in single channel conductance, cannot be measured using SCR. Therefore, the SCR and single GUV methods are complementary.

6. Short summary and outlook

This perspective summarized the information on the interaction of magainin 2 (AMP), lysenin (PFT), and TP10 (CPP) with biological lipid membranes which can be revealed only by the single GUV method. For magainin 2- or lysenin-induced pore formation in lipid membranes, two elementary processes (i.e., the peptide/protein-induced pore formation and the membrane permeation of fluorescent probes through the pores), are observed separately; statistical analysis of the data provides the rate constants of these elementary processes. For the interaction of TP10 with lipid membranes, four elementary processes, i.e., the binding of TP10 to the lipid membrane, the entry of TP10 into a vesicle, TP10-induced pore formation, and the membrane permeation of fluorescent probes through the pores, are observed separately, and the rate constants of all these processes can be determined. Based on the new quantitative information on the elementary processes revealed by the single GUV method, we can begin to elucidate the mechanisms underlying peptide/protein (such as AMP, PFT, and CPP)-induced pore formation and the entry of peptides (such as CPP) into a GUV.

We compared the single GUV method with other methods for investigating the interaction of peptides/proteins with lipid membranes (i.e., the LUV suspension method, the GUV suspension method, and SCR), and discussed the pros and cons of the single GUV method in comparison with the other methods. In conclusion, both the single GUV method and the GUV suspension method are superior to the LUV suspension method, and hence these methods are revealing the interactions of peptides/proteins with lipid membranes. The single GUV method and SCR can provide complementary information.

In future, we can apply the single GUV method to investigate the functions of AMPs, PFTs, CPPs, and various compounds which interact with lipid membranes. The single GUV method provides valuable information on the effects of the mutation of AMP, PFT, and CPP peptides/proteins on membrane permeation, and on the effects of both lipid composition and the physical properties of lipid membranes on membrane permeation. All this information becomes available to the researcher because the single GUV method allows calculation of the rate constants of the elementary processes. This detailed understanding of the elementary processes will greatly contribute to the design of de novo peptides/proteins which mimic the activity of AMP, PFT, CPP and others membrane proteins, and also to the experimental elucidation of the functions of these de novo designed peptides/proteins. The continued development of experimental techniques is indispensable for reducing the time required for single GUV experiments and to increase the accuracy of the calculated rate constants of the elementary processes. Increasing the temporal and spatial resolution of observations using various optical microscopes could allow other elementary processes in various phenomena to be separated and allow their rate constants to be calculated.

References

1. M. Zasloff, *Nature*, 2002, **415**, 389-395.
2. M. N. Melo, R. Ferre, and A. R. B. Castanho, *Nat. Rev. Microbiol.*, 2009, **8**, 1-5.
3. M. Zasloff, *Proc. Natl. Acad. Sci. USA.*, 1987, **84**, 5449-5453.
4. M. Zasloff, B. Martin, and H.-C. Chen, *Proc. Natl. Acad. Sci. U.S.A.*, 1988, **85**, 910-913.
5. D. Wade, A. Boman, B. Wahlin, C. M. Drain, D. Andreu, H. G. Boman, R. B. Merrifield, *Proc. Natl. Acad. Sci. USA.*, 1990, **87**, 4761-4765.
6. M. W. Parker, *Toxicon*, 2003, **42**, 1-6.
7. M. W. Parker, and S. C. Feil, *Prog. Biophys. Mol. Biol.*, 2005, **88**, 91-142.
8. G. Anderluh, and J. Lakey, *Proteins: Membrane binding and pore formation*. Springer-Verlag, Berlin, 2010.
9. M. Magzoub, and A. Gräslund, *Quart. Rev. Biophys.*, 2004, **37**, 147-195
10. M. Zorko, and Ů. Langel, *Adv. Drug. Delivery Rev.*, 2005, **57**, 529-545.
11. F. Madani, S. Lindberg, Ů. Langel, S. Futaki, and A. Gräslund, *J. Biophysics*, 2011, 414729, 10 pages

12. M. Yamazaki, in *Advances in Planar Lipid Bilayers and Liposomes*, ed. A. L. Leitmannova, Elsevier/Academic Press, London. 1988, **7**, 121-142.
13. M. Yamazaki, and T. Ito, *Biochemistry*, 1990, **29**, 1309-1314.
14. K. Matsuzaki, K. Murase, N. Fujii, and K. Miyajima, *Biochemistry*, 1995, **34**, 6521-6526.
15. K. Matsuzaki, K. Sugishita, N. Ishibe, M. Ueha, S. Nakata, K. Miyajima, R. M. Epand, *Biochemistry*, 1998, **37**, 11856-11863.
16. J. M. Boggs, J. Euijung, I. V. Polozov, R. F. Epand, G. M. Anantharamaiah, J. Blazyk, R. M. Epand, *Biochim. Biophys. Acta– Biomembranes*, 2001, **1511**, 28-41.
17. S. M. Gregory, A. Pokorny, P. F. F. Almeida, *Biophys. J.*, 2009, **96**, 116-131.
18. A. Yamaji, Y. Sekizawa, K. Emoto, H. Sakurabe, K. Inoue, H. Kobayashi, and M. Umeda, *J. Biol. Chem.*, 1998, **273**, 5300-5306.
19. A. Yamaji-Hasegawa, A. Makino, T. Baba, Y. Senoh, H. Kimura, S. B. Sato, N. Terada, S. Ohno, E. Kiyokawa, M. Umeda, and T. Kobayashi, *J. Biol. Chem.*, 2003, **278**, 22762-22770.
20. M. Kulma, M. Herec, W. Grudzinski, G. Anderluh, W. I. Gruszecki, K. Kwiatkowska, and A. Sobota, *Biochim. Biophys. Acta– Biomembranes*, 2010, **1798**, 471-481.
21. L. E. Yandek, A. Pokomy, A. Floren, K. Knoeike, Ú. Langel, and P. F. F. Almeida, *Biophys. J.*, 2007, **92**, 2434-2444.
22. E. Barany-Wallje, J. Gaur, P. Lundberg, Ú. Langle, and A. Gräslund, *FEBS Lett*, 2007, **581**, 2389-2393.
23. L. E. Yandek, A. Pokomy, and P. F. F. Almeida, *Biochemistry*, 2008, **47**, 3051-3060.
24. E. Evans, and E. Rawicz, *Phys. Rev. Lett.*, 1990, **64**, 2094-2097.
25. E. Farge, and P. F. Devaux, *Biophys. J.*, 1992, **61**, 347-357.
26. A. Saitoh, K. Takiguchi, Y. Tanaka, and H. Hotani, *Proc. Natl. Acad. Sci. U.S.A.*, 1998, **95**, 1026-1031.
27. T. Tanaka, Y. Tamba, S. M. Masum, Y. Yamashita, and M. Yamazaki, *Biochim. Biophys. Acta– Biomembranes*, 2002, **1564**, 173-182.
28. Y. Yamashita, S. M. Masum, T. Tanaka, T., and M. Yamazaki, *Langmuir*, 2002, **18**, 9638-9641.
29. T. Baumgart, S. T. Hess, and W. W. Webb, *Nature*, 2003, **425**, 821-824.
30. T. Tanaka, and M. Yamazaki, *Langmuir*, 2004, **20**, 5160-5164.

31. T. Tanaka, R. Sano, Y. Yamashita, and M. Yamazaki, *Langmuir*, 2004, **20**, 9526-9534.
32. Y. Tamba, and M. Yamazaki, *Biochemistry*, 2005, **44**, 15823- 15833.
33. Y. Tamba, S. Ohba, M. Kubota, H. Yoshioka, H. Yoshioka, and M. Yamazaki, *Biophys. J.*, 2007, **92**, 3178-3194.
34. Y. Inaoka, and M. Yamazaki, *Langmuir*, 2007, **23**, 720-728.
35. Y. Tamba, and M. Yamazaki, *J. Phys. Chem. B.*, 2009, **113**, 4846-4852.
36. Y. Tamba, H. Ariyama, V. Levadny, and M. Yamazaki, *J. Phys. Chem. B.*, 2010, **114**, 12018- 12026.
37. J. M. Alam, T. Kobayashi, and M. Yamazaki, *Biochemistry*, 2012, **51**, 5160-5172.
38. M. Z. Islam, H. Ariyama, J. M. Alam, and M. Yamazaki, *Biochemistry*, 2014, **53**, 386-396.
39. L. D. Colibus, A. F.-P. Sonnen, K. J. Morris, A. Siebert, P. Abrusci, J. Plitzko, V. Hodnik, M. Leippw, E. Volpi, G. Anderluh, and R. J. C. Gilbert, *Structure*, 2012, **20**, 1498-1507.
40. R. Ishitsuka, and T. Kobayashi, *Biochemistry*, 2007, **467**, 1495-1502.
41. M. Pooga, M. Hällbrink, M. Zorko, and Ü. Langel, *FASEB. J.*, 1998, **12**, 67-77.
42. M. Pooga, C. Kut, M. Kihlmark, M. Hällbrink, S. Fernaeus, R. Raid, T. Land, E. Hallberg, T. M. Bartfai, and Ü. Langel, *FASEB. J.*, 2001, **15**, 1451-1453.
43. U. Soomets, M. Lindgren, X. Gallet, M. Pooga, M. Hällbrink, A. Elmquist, L. Balaspiri, M. Zorko, M. Pooga, R. Brasseur, and Ü. Langel, *Biochim. Biophys. Acta– Biomembranes*, 2000, **1467**, 165-176.
44. S. E.L.–Andaloussi, H. Johansson, A. Magnúsdóttir, P. Järver, P. Lundberg, and Ü. Langel, *J. Control Release*, 2005, **110**, 189-201.
45. P. Walde, K. Cosentino, H. Engel, and P. Stano, *ChemBioChem*, 2010, **11**, 848-865.
46. S. Pautot, B. J. Frisken, D. A. Weitz, *Langmuir*, 2003, **19**, 2870-2879.
47. Y. Yamashita, M. Oka, T. Tanaka, and M. Yamazaki, *Biochim. Biophys. Acta–Biomembranes*, 2002, **1561**, 129-134.
48. Y. Tamba, H. Terashima, and M. Yamazaki, *Chem. Phys. Lipids*, 2011, **164**, 351-358.
49. B. Bechniger, M. Zasloff, and S. J. Opella, *Protein Sci.* 1993, **2**, 2077-2084.
50. D. J. Hirsh, J. Hammer, W. L. Maloy, J. Blazyk, and J. Schaefer, *Biochemistry*, 1996, **35**, 12733-12741.
51. K. Matsuzaki, O. Murase, N. Fujii, and K. Miyajima, *Biochemistry*, 1996, **35**, 11361-11368.

52. L. T. Yang, M. Weiss, R. I. Lehrer, and H. W. Huang, *Biophys. J.* 2000, **79**, 2002-2009.
53. S. Qian, W. Wang, L. Yang, and H. W. Huang, *Proc. Natl. Acad. Sci. USA.* 2008, **105**, 17379-17383.
54. A. S. Ladokhin, W. C. Wimley, and S. H. White, *Biophys. J.* 1995, **69**, 1964-1971.
55. S. M. Gregory, A. Cavanaugh, V. Journigan, A. Pokorny, and P. F. F. Almeida, *Biophys. J.* 2008, **94**, 1667-1680.
56. P. F. Almeida, and A. Pokorny, *Biochemistry*, 2009, **48**, 8083-8093.
57. J. Israerachvili, *Intermolecular & Surface Forces*, 2 nd ed. Academic Press, New York. 1992. Chap. 12, pp. 213-259.
58. S. McLaughlin, *Annu. Rev. Biophys. Biophys. Chem.* 1989, **18**, 113-136.
59. S. J. Li, Y. Yamashita, and M. Yamazaki, *Biophys. J.*, 2001. **81**, 983-993.
60. Y. Okamoto, S. M. Masum, H. Miyazawa, and M. Yamazaki, *Langmuir*, 2008. **24**, 3400-3406.
61. S. J. Ludtke, K. He, K. H. Heller, T. A. Harroun, L. Yang, and H. W. Huang, *Biochemistry*, 1996, **35**, 13723-13728.
62. G. Fuertes, A. Garcia-Sáez, S. Esteban-Martin, D. Giménez, O. L. Sánchez-Muñoz, P. Schwille, and J. Salgado, *Biophys. J.*, 2010, **99**, 2917-2925.
63. S. Bleicken, O. Landeta, A. Landajuela, G. Basañez, and A. J. García-Sáez, *J. Biol. Chem.*, 2013, **288**, 33241-33252.
64. T. Aoki, M. Hirano, Y. Takeuchi, T. Kobayashi, T. Yanagida, and T. Ide, *Proc. Jpn. Acad. Ser. B.* 2010, **86**, 920-925.
65. P. Schön, A. J. Garcia-Saez, P. Malovrh, K. Bacia, G. Anderluh, and P. Schwille, *Biophys. J.*, 2008, **95**, 691-698.
66. P. E. G. Thorén, D. Persson, M. Karlsson, and B. Nordén, *FEBS Lett.*, 2000, **482**, 265-268.
67. A. Mishra, G. H. Lai, N. W. Schmidt, V. Z. Sun, A. R. Rodriguez, R. Tong, L. Tang, J. Cheng, T. J. Deming, D. T. Kamei, and G. C. L. Wong, *Proc. Natl. Acad. Sci. U.S.A.*, 2011, **108**, 16883-16888.
68. S. A. Wheaten, F. D. O. Ablan, B. L. Spaller, J. M. Trieu, and P. F. Almeida, *J. Amer. Chem. Soc.*, 2013, **135**, 16517-16525.

69. T. Maeda, and S. Ohnishi, *FEBS Lett.*, 1980, **122**, 283-287.
70. V. Levadny, T. Tsuboi, M. Belaya, and M. Yamazaki, *Langmuir*, 2013, **29**, 3848-3852.
71. H. Bayley, L. Jayasinghe, and M. Wallace, *Nat. Struct. Mol. Biol.* 2005, **12**, 385-386.
72. E. A. Ambroggio, F. Separovic, J. H. Bowie, C. D. Fidelio, and L. A. Bagatolli, *Biophys. J.* 2005, **89**, 1874-1881.
73. B. Apellániz, J. L. Nieva, P. Schwille, and A. J. García-SâG. Fuertes, and A. J. García-Sâez, *Biophys. J.*, 2010, **99**, 3619-3628.
74. C. L. Bergstrom, P. A. Beales, Y. Lv, T. K. Vanderlick, and J. T. Groves, *Proc. Natl. Acad. Sci. U.S.A.*, 2013, **110**, 6269-6274.
75. B. Sakmann, and E. Neher, eds. *Single-Channel Recording*, Plenum Press, New York, 1983.
76. B. Hill, *Ionic Channels of Excitable Membranes*, 2nd ed., Sinauer Associates, Sunderland, MA, 1992
77. M. Oblatt-Montal, M. Yamazaki, R. Nelson, and M. Montal, *Protein Science*, 1995, **4**, 1490-1497.
78. S. M. Bezrukov, and I. Vodyanoy, *Nature*, 1995, **378**, 362-364.
79. E. M. Nestorovich, C. Danelon, M. Winterhalter, and S. M. Bezrukov, *Proc. Natl. Acad. Sci. U.S.A.*, 2002, **99**, 9789-9794.

Acknowledgement

This work was supported in part by a Grant-in-Aid for Scientific Research (B) (No. 21310080 and 17310071) from the Japan Society for the Promotion of Science (JSPS) to M.Y., and also by a Grant-in-Aid for Scientific Research in Priority Area (System Cell Engineering by Multi-scale Manipulation) (No. 18048020 and 20034023) and that in Priority Area (Soft Matter Physics) (No. 21015009 and 19031011) from the Ministry of Education, Culture, Sports, Science and Technology (MEXT) of Japan to M.Y. This work was partially carried out using instruments at the Center for Instrumental Analysis, Shizuoka University.

Table 1: Rate constants of 7 μM magainin 2-induced membrane permeation of various fluorescent probes in single 50%DOPG/50%DOPC-GUVs with a radius of $5 \pm 1 \mu\text{m}$ at 25 °C. (A) at the initial stage, and (B) at the final steady stage. Reprinted from ref. 36 with permission from the American Chemical Society.

Fluorescent probes	R_{SE} nm	Mode of leakage	Initial stage (s^{-1})	Final steady stage (s^{-1})
TRD-3k	1.4	two phases	$(1.9 \pm 0.1) \times 10^{-1}$	$(1.0 \pm 0.1) \times 10^{-2}$
TRD-10k	2.7	two phases	$(8.2 \pm 0.8) \times 10^{-2}$	$(3.3 \pm 0.4) \times 10^{-3}$
AF-SBTI	2.8	Initial leakage	$(1.2 \pm 0.1) \times 10^{-1}$	No leakage
TRD-40k	5.0	initial leakage	$(4.0 \pm 0.3) \times 10^{-2}$	No leakage
FITC-BSA	3.6	initial leakage	$(4.8 \pm 0.3) \times 10^{-2}$	No leakage

Figure Captions

Fig. 1: A schematic diagram of the principles behind the single GUV method.

Fig. 2: Membrane permeation of calcein from single 60%DOPG/40%DOPC-GUVs induced by magainin 2 in buffer A (10 mM PIPES, pH 7.0, 150 mM NaCl, 1 mM EGTA). (A) Fluorescence images (2) show that the calcein concentration inside the GUV progressively decreased after the addition of 3 μM magainin 2. The numbers above each image show the time in seconds after magainin 2 addition was started. Also shown are phase contrast images of the GUV at time 25 (1) and at 255 s (3). The bar corresponds to 10 μm . (B) Time course of the change in the normalized fluorescence intensity of the GUV shown in (A). (C) Other examples of the change in fluorescence intensity of single GUVs over time under the same conditions as in (A). (D) Schematic presentation of the two-state transition from the binding state to the pore state induced by magainin 2. (E) Time course of P_{intact} of 60%DOPG/40%DOPC-GUV in the presence of various concentrations of magainin 2: (\circ) 5, (\blacksquare) 3, (Δ) 2.5, and (\bullet) 1 μM . The solid lines represent the best fit curves of eq. 1. The obtained values of k_p were 5.9×10^{-2} , 1.7×10^{-2} , and $9.5 \times 10^{-3} \text{ s}^{-1}$ for 5, 3, and 2.5 μM magainin 2, respectively. Figs. 2A–C and E are reprinted from ref. 35 with permission from the American Chemical Society.

Fig. 3: Dependence of the rate constant of pore formation, k_p , on magainin 2 concentration in buffer A, $C_{\text{eq}}^{\text{mag}}$. (A) Dependence of k_p on $C_{\text{eq}}^{\text{mag}}$. (\blacksquare): 60%DOPG/40%DOPC-, (green \bullet): 50%DOPG/50%DOPC-, (blue \bullet): 40%DOPG/ 60%DOPC-, and (red \blacktriangle): 30%DOPG/70%DOPC-GUVs. Two to four independent experiments for a given magainin 2 concentration were conducted using 30–40 single GUVs in each experiment for 40%DOPG/60%DOPC- and 30%DOPG/70%DOPC-GUVs, and using 10–20 single GUVs in each experiment for 60%DOPG/40%DOPC- and 50%DOPG/50%DOPC-GUVs and obtained the average values and standard errors of k_p . (B) Dependence of k_p on X . Fig. 3B was obtained by replotting the graphs of the dependence of k_p on $C_{\text{eq}}^{\text{mag}}$ (Fig. 3A) using the estimated values of $K_{\text{int}}^{\text{mag}}$. (blue \bullet): 40%DOPG/60%DOPC-, and (red \blacktriangle): 30%DOPG/70%DOPC-GUVs. Reprinted from ref. 35 with permission from the American Chemical Society.

Fig. 4: Membrane permeation of various-sized water-soluble fluorescent probes through a magainin 2-induced pore in a membrane. (A) Schematic presentation of the membrane permeation of compounds through a pore in a lipid membrane. (B) (C) Membrane permeation of TRD-10k from single 50%DOPG/50%DOPC-GUVs induced by magainin 2 in buffer A at 25 °C. Time course of the change in the normalized fluorescence intensity of several “single GUVs” induced by (B) 7 μM , and (C) 4 μM magainin 2. (D) Time course of the logarithm of the normalized fluorescence intensity, FI , of single 50%DOPG/50%DOPC-GUVs containing TRD-3k or TRD-10k during the interaction of 4 μM magainin 2 with single GUVs. Figs (B)–(D) are reprinted from ref. 36 with permission from the American Chemical Society.

Fig. 5: Membrane permeation of calcein from single SM/DOPC/chol (42/30/28)-GUVs induced by lysenin in PBS (1.5 mM KH_2PO_4 , 8.1 mM Na_2HPO_4 , 137 mM NaCl, 2.7 mM KCl) at 37 °C. (A) Fluorescence images (2) show that the calcein concentration inside the GUV progressively decreased during the addition of 40 ng/mL lysenin. The numbers below each image show the time in seconds after lysenin addition was started. Also shown are phase-contrast images of the GUV at time 0 s (1) and at 602 s (3). The bar corresponds to 20 μm . (B) Time course of the change in FI of the inside of the GUV shown in (A). (C) Dependence of P^s [$\mu\text{m/s}$] on lysenin concentration (C [ng/mL]). The relationship between P^s and C was plotted for SM/DOPC/chol (42/30/28)-GUVs (red \bullet) and SM/DOPC (58/42)-GUVs (blue \blacksquare). The bars indicate standard errors. (D) SDS-resistant oligomerization of lysenin in the presence of lipid membranes containing SM. A lysenin solution (187 nM) was incubated with SM/DOPC (58/42)-SUVs or SM/DOPC/chol (42/30/28)-SUVs at various SM/lysenin molar ratios (20–20000 and 17–17000, respectively) for 5 min at 37 °C. The samples were then analyzed by SDS-PAGE (silver staining). The lysenin monomer and oligomer are indicated by M and O, respectively. (E) The dependence of the SDS-resistant oligomer fraction on the SM/lysenin molar ratio shown in (D); SM/DOPC/chol (42/30/28)-SUVs (red \bullet) and SM/DOPC (58/42)-SUVs (blue \blacksquare). The bars indicate standard errors. (F) Phase separation of lipid membranes between the l_o and l_d phases in SM/DOPC/chol (42/30/28)-GUVs. The domains with high fluorescence intensity correspond to the l_d phase. The bars correspond to 20 μm . Figs (A)–(E) are reprinted from ref. 37 with permission from the American Chemical Society.

Fig. 6: Membrane permeation of calcein from single SM/chol (60/40)-GUVs induced by lysenin at 37 °C. (A) Fluorescence images (2) show that the calcein concentration inside the GUV progressively decreased during the addition of 40 ng/mL lysenin. The numbers below each image show the time in seconds after the lysenin addition was started. Also shown are phase contrast images of the GUV at time 0 s (1) and at 690 s (3). The bar corresponds to 10 μm . (B) Time course of the change in FI of the inside of the GUV. (C) Dependence of P^s [$\mu\text{m/s}$] on lysenin concentration (C [ng/mL]). The relationship between P^s and C is plotted for SM/chol (60/40)-GUVs (green \blacktriangle). The bars indicate the standard error. For comparison, the same relationship was also plotted for the SM/DOPC/chol (42/30/28)-GUVs (red \bullet) shown in Fig. 5C. (D) The dependence of the SDS-resistant oligomer fraction of lysenin on the SM/lysenin molar ratio shown in (A); SM/chol (60/40)-SUVs (green \blacktriangle) and SM/DOPC/chol (42/30/28)-SUVs (red \bullet). The bars indicate standard errors. (E) Dependence of k_p on lysenin concentration in PBS. (red \bullet) SM/DOPC/chol (42/30/28)-, and (green \blacktriangle) SM/chol (60/40)-GUVs. Two to three independent experiments were conducted for a given lysenin concentration using 10-20 single GUVs in each experiment and obtained the average values and standard errors of k_p . Reprinted from ref. 37 with permission from the American Chemical Society.

Fig. 7: Membrane permeation of AF647 and entry of CF-TP10 into single 20%DOPG/79%DOPC/ 1%biotin-lipid-GUVs containing smaller vesicles, induced by 1.9 μM CF-TP10. (A) CLSM images of (1) AF647 and (2) CF-TP10. The numbers above each image show the time in seconds after CF-TP10 addition was started. The bar corresponds to 30 μm . (B) Time course of the change in normalized fluorescence intensity of the GUV shown in (A). Red and green points correspond to the fluorescence intensity of AF647 inside the GUV and of CF-TP10 in the rim of the GUV, respectively. (C) Dependence of the fraction of entry of CF-TP10 before pore formation on the concentration of CF-TP10 (green \bullet). For comparison, the dependence of the fraction of leaked GUV after 6 min interaction on the concentration of CF-TP10 is shown (red \square). (D) The dependence of the rate constant of CF-TP10- (or TP10)-induced pore formation in 20%DOPG/79%DOPC/1%biotin-lipid membranes on concentration. TP10 (green \bullet) and CF-TP10 (red \square). The rate constant of CF-TP10-induced pore formation was obtained by the analysis of the leakage of AF647 and that of TP10-induced pore formation was obtained by analysis of the leakage of calcein. The average values and standard errors of k_p were obtained. Reprinted from ref. 38 with permission from the American Chemical Society.

Fig. 8: Membrane permeation of AF647 and penetration of CF-TP10 in single 20%DOPG/79%DOPC/ 1% biotin-lipid-GUVs induced by 1.9 μM CF-TP10. (A) Time course of the change in normalized fluorescence intensity of the GUV. Red and green points correspond to the fluorescence intensity of AF647 inside the GUV and of CF-TP10 in the rim of the GUV, respectively. The solid black line represents the best fit curve using eq. (3). The obtained value of k_{app} was 0.026 s^{-1} . (B) Dependence of k_{app} on CF-TP10 concentration. The time course of the change in the fluorescence intensity of 15–25 GUVs with a diameter of 30–40 μm was measured. The average values and standard errors of k_{app} were obtained. The solid blue line represents the best fit curve using eq. (4). Reprinted from ref. 38 with permission from the American Chemical Society.

Fig. 1

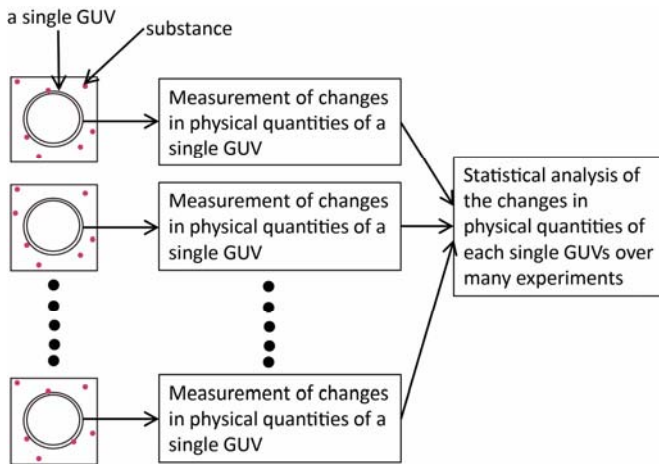


Fig. 2

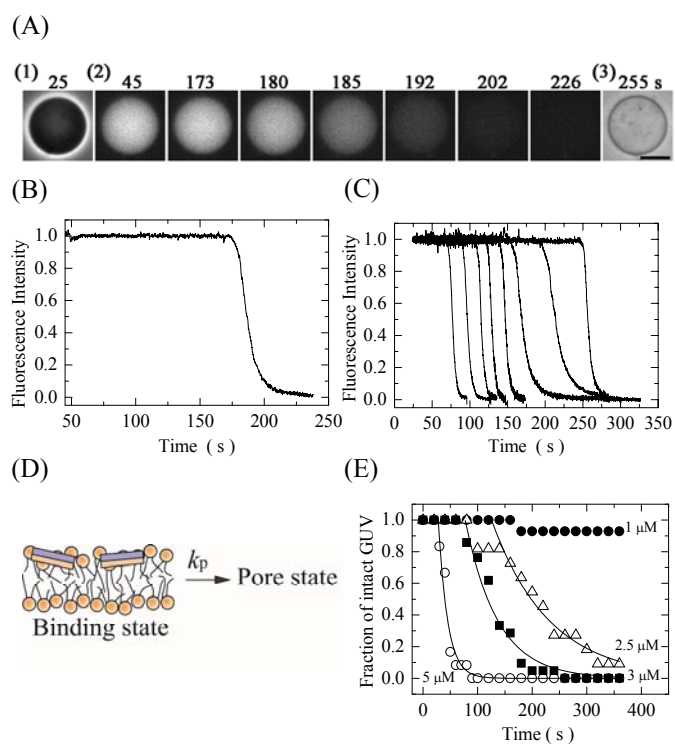


Fig. 3

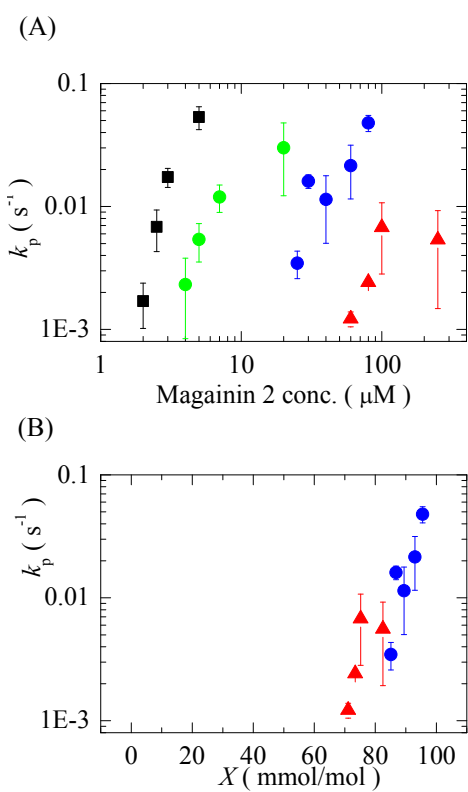


Fig. 4

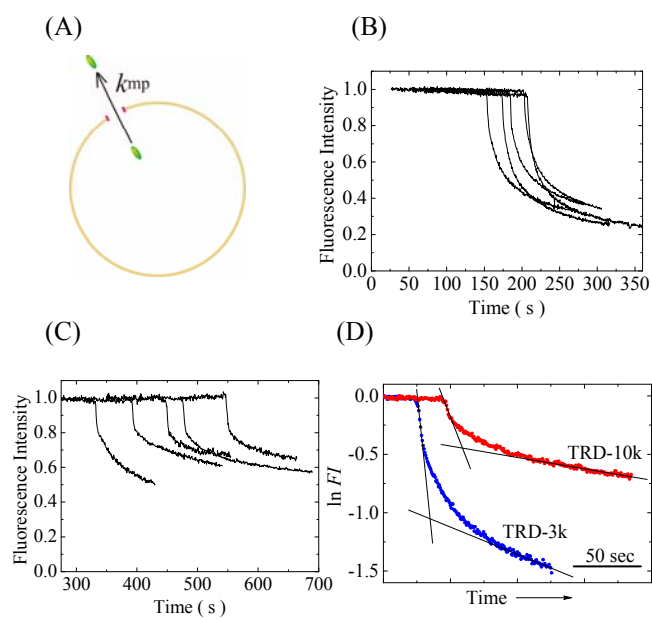


Fig. 5

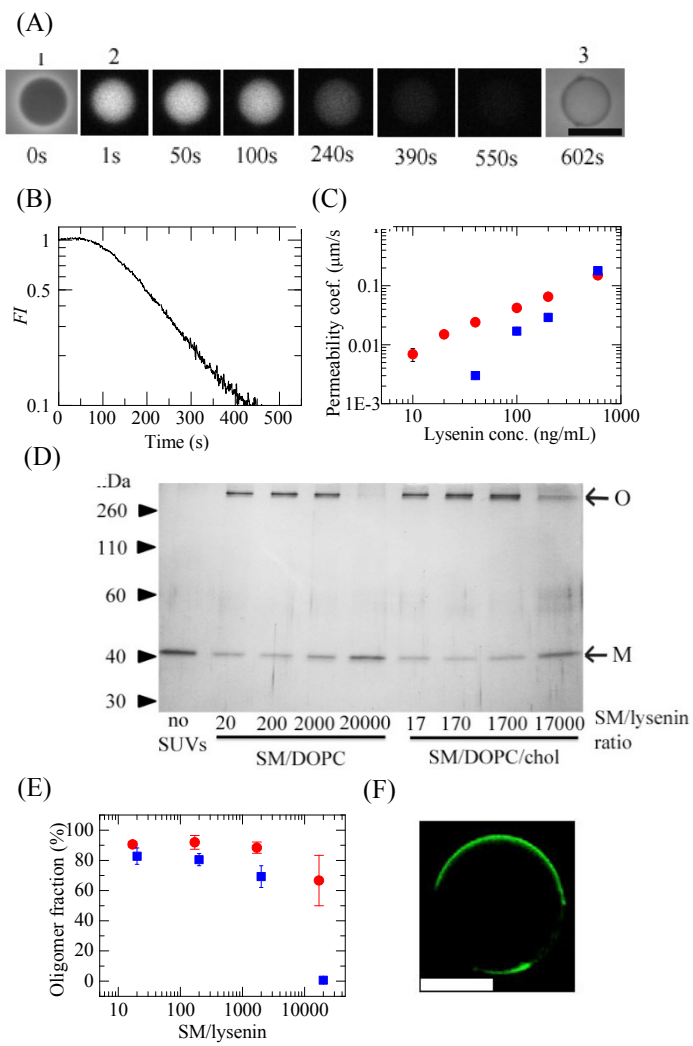


Fig. 6

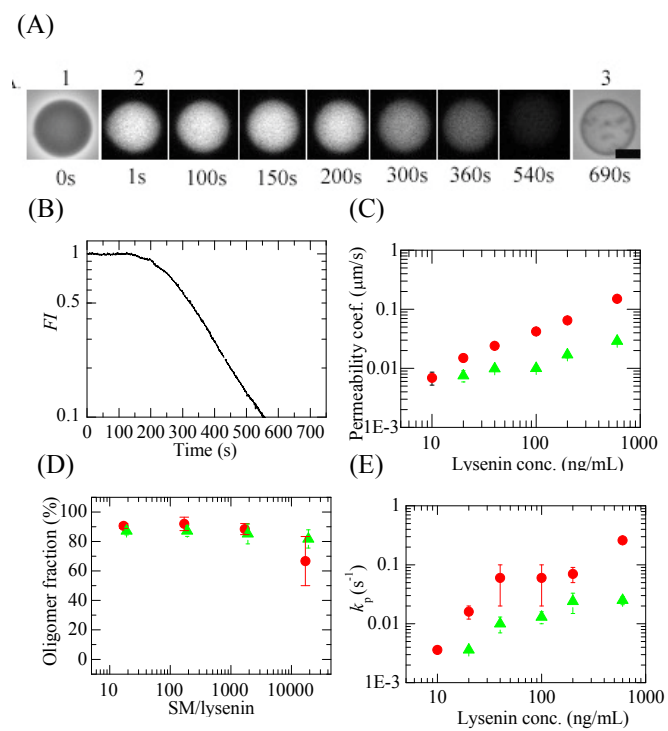


Fig. 7

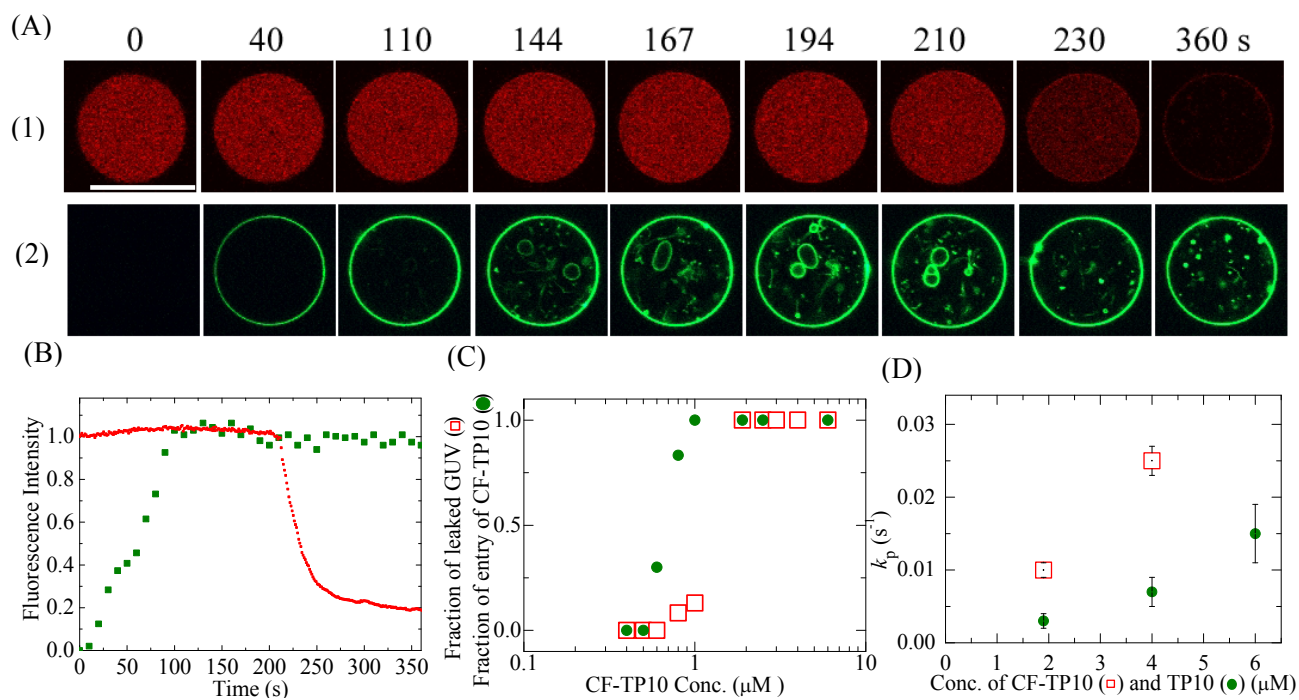
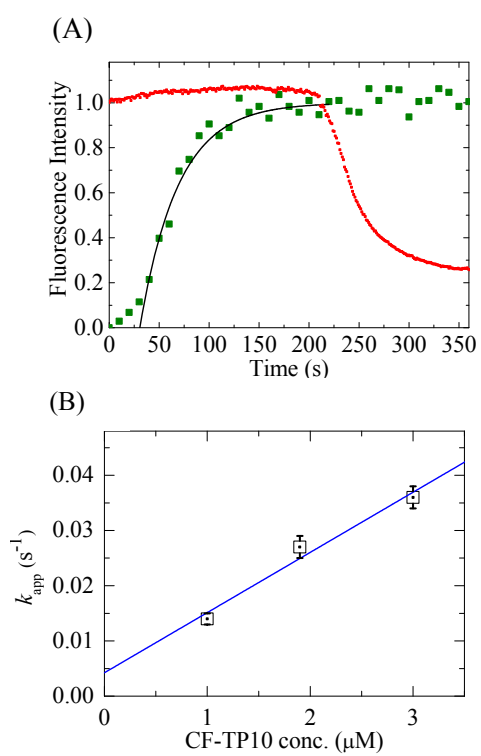


Fig. 8



CV of all the authors

Md. Zahidul Islam is currently a PhD student at Graduate School of Science and Technology, Shizuoka University, Japan. He received his MS degree in 2003 from Khulna University, Bangladesh. From 2003 to 2012, he worked in pharmaceutical company. His research interest is to reveal the mechanism or mode of action of cell penetrating peptide on lipid bilayer by the single GUV method.



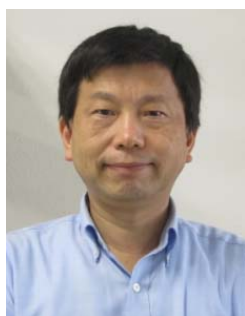
Jahangir Md. Alam is a post-doctoral fellow in Research Institute of Electronics, Shizuoka University, Japan. Concurrently he is a lecturer at the Faculty of Applied Science and Technology, Islamic University, Bangladesh. He received his PhD from the Shizuoka University in 2013. His research interest is to reveal the mechanism of the pore formation induced by pore-forming toxin and antimicrobial peptides.



Yukihiro Tamba is currently an associate professor of physics at Suzuka National College of Technology, Japan. He received his PhD from Shizuoka University, Japan in 2005. His research interest is to develop a new imaging system for the single GUV method and also to reveal the mechanism of the interaction of flavonoids with lipid membranes.



Mohammad Abu Sayem Karal is currently a PhD student at Graduate School of Science and Technology, Shizuoka University, Japan. He is an Assistant Professor, Department of Physics, Bangladesh University of Engineering and Technology (BUET), Bangladesh. He received his MS degree in 2002 from University of Dhaka, Bangladesh. His current research interest is peptide and tension-induced pore formation on giant liposomes and understanding their biophysical phenomena.



Masahito Yamazaki is currently a professor at Research Institute of Electronics, Shizuoka University, Japan. He is also a professor at Dept. Physics, Graduate School of Science, and at Dept. Integrated Bioscience, Graduate School of Science and Technology, Shizuoka University. He received his PhD from Kyoto University. His research interest is to develop new imaging methods for investigation of structures, functions, and dynamics of biomembranes and cells, and to reveal their elementary processes and mechanisms.